Single-component reflecting objective for low-temperature spectroscopy in the entire visible region

Fujiyoshi, Satoru; Fujiwara, Masanori; Kim, Changman; Matsushita, Michio; van Oijen, Antonius; Schmidt, Jan

Published in:
Applied Physics Letters

DOI:
10.1063/1.2767778

Single-component reflecting objective for low-temperature spectroscopy in the entire visible region

Satoru Fujiyoshi,[a] Masanori Fujiwara, Changman Kim, and Michio Matsushita
Department of Physics, Tokyo Institute of Technology, Meguro, Tokyo, 152-8551, Japan and PRESTO, JST, Tokyo, Japan

Antoine M. van Oijen
Department of Biological Chemistry and Molecular Pharmacology, Harvard Medical School, 250 Longwood Avenue, SGM204A, Boston, Massachusetts 02115

Jan Schmidt
Huygens Laboratory, P.O. Box 9504, 2300 RA Leiden, The Netherlands

(Received 5 June 2007; accepted 10 July 2007; published online 2 August 2007)

A single-component reflecting objective was constructed for low-temperature spectroscopy with optimal imaging and transmission properties at all visible wavelengths. The performance of the objective immersed in superfluid helium at a temperature of 1.5 K was tested by comparing dark-field images of uncolored polymer beads taken at wavelengths of 400 and 800 nm. Under conditions optimized for imaging at both wavelengths, the size of the image is <1.3 times of the diffraction limit. The objective collects emission from a point source at focus with a solid angle of 0.32π sr. © *2007 American Institute of Physics*. [DOI: 10.1063/1.2767778]

To observe weak optical signals, it is essential to collect photons using a large solid angle of detection. In low-temperature experiments, one of the methods to fulfill this requirement is to place an objective with a high numerical aperture (NA) in a liquid-helium cryostat in the vicinity of a sample.[1] In addition to achieving a large solid angle in the detection path, this configuration enables high stability of the position of the objective relative to the sample and allows for signal acquisition over several hours.[2] However, imaging at low temperature often suffers from chromatic aberration because chromatically corrected, multicomponent objectives typically cannot withstand cooling to liquid-helium temperature. The aberration becomes even more severe in two-photon and ultraviolet fluorescence spectroscopy and microscopy. A straightforward solution to chromatic aberration is to use reflecting optics.[3–5] Here, we report the construction and the performance of a single-component reflecting objective for low-temperature spectroscopy. The objective consists of two concentric concave and convex mirrors. To maintain a rigid alignment of the mirrors at low temperature, the entire objective is constructed from a single piece of fused silica. At liquid-helium temperature, the axial chromatic aberration of the objective was smaller than the focal depth at the entire visible wavelengths ranging from 400 to 800 nm.

As a light source the fundamental and second harmonic output of a femtosecond Ti:sapphire oscillator laser was used (repetition rate of 90 MHz, pulse width of 140 fs at wavelength of 800 nm). The samples were spin-coated aqueous solutions of polystyrene beads (Polysciences; the diameter of 200 nm) on fused silica plates (spinning at 2000 rpm for 2 min).

Figure 1(a) shows the cross section of the single-component reflecting objective. Fused silica was chosen as a material because of the high transparency over the entire visible and ultraviolet regions and its small thermal expansion coefficient. The objective has a rotational symmetry along the optical axis labeled as z. Convex and concave spherical surfaces with radii of R_1 and R_2 are centered at O_M. Both these surfaces were coated with aluminum. In a Cas-

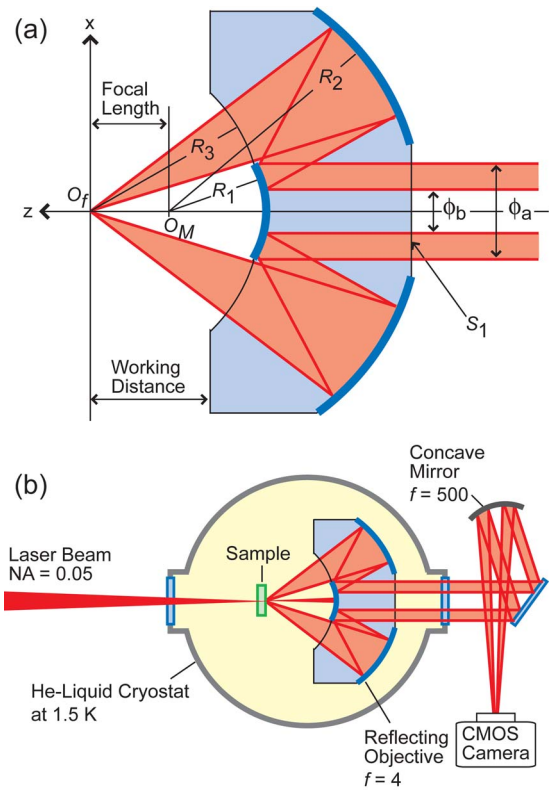

FIG. 1. (Color online) (a) Cross section of the single-component reflecting objective. The focal length is 4 mm, NA is 0.6, and the working distance is 6 mm. Symbols used in the figure: R_1 and R_2, the radii of the spherical mirrors; R_3, the radius of the polished spherical surface; S_1, the polished flat surface; O_f, the focus of the objective and the center of the curvature of R_3; O_M, the center of the curvatures of R_1 and R_2; ϕ_a and ϕ_b, the outer and inner diameters of the output light. (b) Optical and cryogenic apparatus used for dark-field imaging of polymer beads at a temperature at 1.5 K.

[a]Electronic mail: fujiyoshi@phys.titech.ac.jp

segrain objective, the ratio between R_1, R_2, and the focal length is $\sqrt{5}-1:\sqrt{5}+1:1$, which nullifies the lowest order of spherical aberration. With this condition, the distance between the focus of the objective (O_f) and O_M is equal to the focal length. A spherical surface with a radius of R_3 is centered at O_f. This spherical surface and a flat surface of S_1 were polished and coated with a magnesium fluoride antireflective coating. The focal length and NA were set to be 4 mm and 0.6. Consequently the radii of R_1, R_2, and R_3 are 4.944, 12.944, and 8.659 mm, respectively. The mirror with R_1 blocks the center of the signal light. Thus, the collimated output light is of a donut shape with ϕ_a and ϕ_b of 4.8 and 2.2 mm. The solid angle with which the objective collects emission from a point source at the focus is 0.32π sr. This solid angle is 20% smaller than the solid angle corresponding to NA of 0.6 (0.40π sr). The objective with specific dimensions and precision requirements was custom made by lens-making companies (Sankyo Optics Industry and Optonexus).

The key feature of the reflecting objective is the design of the R_3 and S_1 surfaces. A spherical wave emanating from a point source at O_f crosses the spherical surface of R_3 at normal angle. As a consequence, the spherical wave is not refracted at the interface of R_3. The pair of the concave and convex mirrors collimates the spherical wave. The collimated wave crosses S_1 at normal angle and is not refracted at the helium-silica interface. On the other hand, the light from a point source that is laterally shifted from the optical axis is refracted at the surface of R_3 to a transmission angle that depends on the wavelength-dependent index of refraction. However, a calculation guarantees that the wavelength dependence of the lateral position of the image is much smaller than the spot size because of a compensation of the first refraction by the second one.[6]

Dark-field imaging at liquid-helium temperature (1.5 K) is achieved as follows [Fig. 1(b)]: Both the reflecting objective and a sample were immersed into a liquid-helium bath. The position of the objective relative to the sample was stable within the focal depth for more than 5 h. The axial and lateral positions of the sample can be controlled from outside the cryostat. The laser beam with a wavelength of λ was focused by low NA optics (NA of 0.05) onto the backside of the sample. The transmitted excitation beam was blocked by the mirror R_1. Signal light was collected and collimated by the objective, and focused with a concave mirror (the focal length of 500 mm) onto a complementary metal oxide semiconductor camera with a resolution of 1280 pixels $\times$1024 pixels and a detector size of 6.66×5.32 mm^2.

Before testing the performance of the objective at liquid-helium temperature, it was characterized at room temperature (296 K). Dark-field imaging of polymer beads with a diameter of 200 nm was carried out at λ=400 nm [Fig. 2(a)] and λ=800 nm [Fig. 2(b)]. Since the polymer beads do not contain dyes and their absorption wavelength is far from the laser wavelengths, the signals imaged in Figs. 2(a) and 2(b) are caused by scattering and refraction. The alignment of the objective with respect to the sample was kept intact during measurements at the two different wavelengths. In the images at λ=400 and 800 nm, the disk and rings appeared symmetric. The full width at half maximum (FWHM) of the disks was 0.40 μm at λ=400 nm and 0.74 μm at λ=800 nm. The lateral resolution of the objective at room temperature is 1.3 and 1.2 times, respectively, larger than the theoretical values, 0.31 μm at λ=400 nm and 0.62 μm at

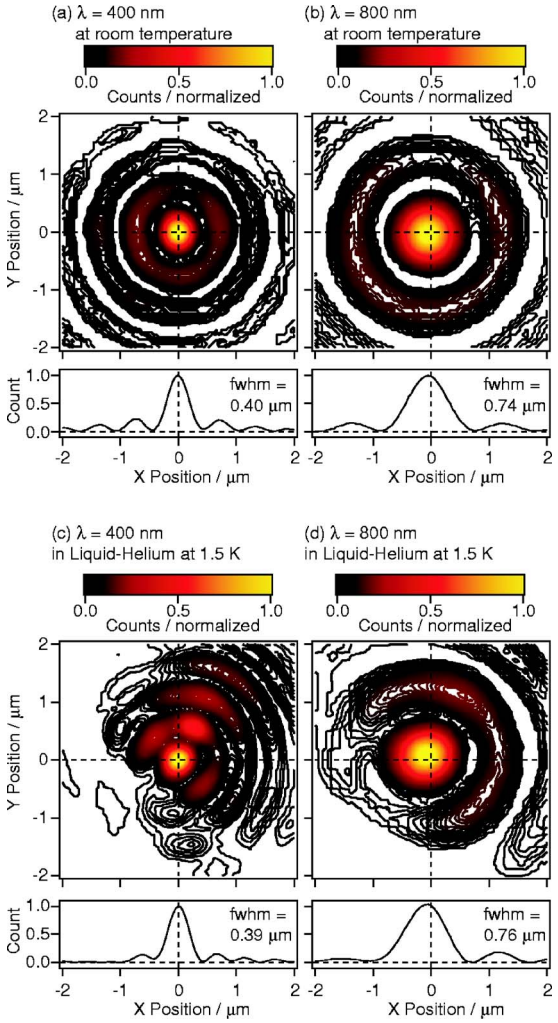

FIG. 2. (Color online) Dark-field images of a polymer bead and their cross sections at $y=0$ μm. The images of (a) and (b) were taken at 296 K and (c) and (d) at 1.5 K. At each temperature, two different wavelengths were employed, λ=400 nm for (a) and (c) and λ=800 nm for (b) and (d). The alignment of the objective with respect to the sample was kept intact when the wavelength was changed. The FWHM of the central disk is indicated in the figures.

λ=800 nm, which are determined from the Fourier transform of the collimated light with ϕ_a and ϕ_b of Fig. 1(a). Since the measurements at the two different wavelengths were performed at the same axial position, the result clearly shows that the axial chromatic aberration is smaller than the focal depth. By comparing the centers of the images, the lateral shift of the disks by changing λ from 400 to 800 nm was 0.07 μm, much smaller than the spot sizes.

The imaging properties of the objective at low temperature are similar to those at room temperature. The asymmetry of the peripheral rings of the images in Figs. 2(c) and 2(d) is caused by a thermal distortion of the objective forced by its holder. However, the central disk is as symmetrical as at room temperature. The ellipticity in liquid helium was 0.93 (λ=400 nm) and 0.96 (λ=800 nm), and at room temperature 0.87 (λ=400 nm) and 0.98 (λ=800 nm). The size of the central disk is the same as at room temperature within the experimental error. The FWHM of the central disk was 0.39 μm at λ=400 nm and 0.76 μm at λ=800 nm. At the position optimal for focusing the image at both wavelengths, the size of the image is less than 1.3 times of the diffraction limit. The lateral shift of the disks of 0.13 μm by changing λ

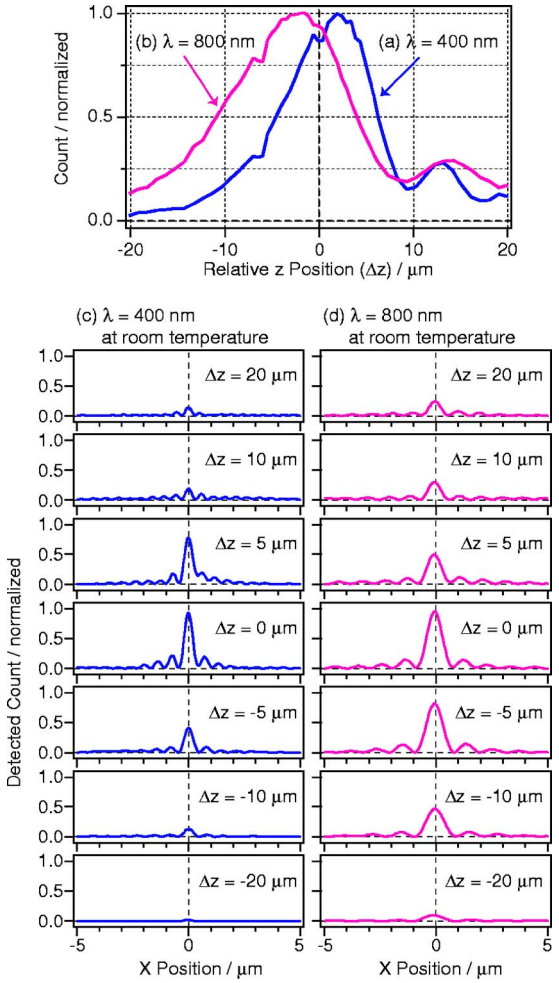

FIG. 3. (Color online) Axial chromatic aberration of the single-component reflecting objective measured at room temperature (296 K). From the images of a polymer bead, intensity contained in the circle having a diameter of 2λ centered at $x=y=0$ μm is plotted as a function of Δz [(a) and (b)]. Cross section of the image at $y=0$ μm is shown at several different Δz at λ=400 nm (c) and 800 nm (d).

from 400 to 800 nm is smaller than the spot size. In summary any chromatic aberration at low temperature has a minimal impact on the imaging quality.

The axial chromatic aberration was quantified in air atmosphere at room temperature. The image was measured as a function of the position of the objective relative to the sample (Δz). From each image, the intensity contained in the circle having a diameter of 2λ centered at $x=y=0$ μm was integrated and plotted against Δz. The resultant two curves taken at the two wavelengths are shown in Figs. 3(a) and 3(b). The peak and width of the curves correspond to the focal position and depth, respectively. The distance between the focal positions at λ=400 nm and λ=800 nm amounts to 4 μm, but is significantly smaller than the focal depth, which is 11 μm at λ=400 nm and 15 μm at λ=800 nm. For comparison, this distance amounts to approximately 170 μm for an aspheric singlet with a focal length and a numerical aperture comparable to our reflective objective (Thorlabs, C671TME-A; focal length of 4.02 mm, NA of 0.6). The cross section of the image at $y=0$ μm as a function of Δz is shown in Figs. 3(c) and 3(d). The spots at λ=400 and λ=800 nm are optimally focused simultaneously at $\Delta z=0$ μm, at which position the images in Figs. 2(a) and 2(b) were obtained.

In conclusion, we demonstrate that a single-component reflecting objective is capable of high-NA imaging at liquid-helium temperature in the entire visible region, making it suitable for low-temperature spectroscopy. The application of this objective can be easily extended to two-photon and ultraviolet fluorescence spectroscopy and microscopy at low temperature, either in superfluid helium or in cold helium gas.

This work was supported by Grant-in-Aids for Young Scientists (B) from the Ministry of Education, Culture, Sports, Science Technology of Japan (No. 17750006), Grant-in-Aid for Scientific Research (B) from JSPS (No. 16340121), the Sumitomo Foundation, and the Asahi Glass Foundation.

[1]W. E. Moerner and M. Orrit, Science **283**, 1670 (1999).
[2]A. Bloess, Y. Durand, M. Matsushita, H. van der Meer, G. J. Brakenhoff, and J. Schmidt, J. Microsc. **205**, 76 (2002).
[3]J. Jasny, J. Sepiol, T. Irngartinger, M. Traber, A. Renn, and U. P. Wild, Rev. Sci. Instrum. **67**, 1425 (1996).
[4]C. Brunel, B. Lounis, P. Tamarat, and M. Orrit, Phys. Rev. Lett. **83**, 2722 (1999).
[5]A. Drechsler, M. A. Lieb, C. Debus, A. J. Meixner, and G. Tarrach, Opt. Express **9**, 637 (2001).
[6]M. Fujiwara, S. Fujiyoshi, M. Matsushita, A. M. van Oijen, and J. Schmidt (unpublished).